



## Testing the dual-route model of perceived gaze direction: Linear combination of eye and head cues.

Otsuka, Y; Mareschal, I; Clifford, CW

This work is licensed under a Creative Commons Attribution-NonCommercial-NoDerivatives 4.0 International License.

For additional information about this publication click this link.

<http://qmro.qmul.ac.uk/xmlui/handle/123456789/16021>

Information about this research object was correct at the time of download; we occasionally make corrections to records, please therefore check the published record when citing. For more information contact [scholarlycommunications@qmul.ac.uk](mailto:scholarlycommunications@qmul.ac.uk)

# Testing the dual-route model of perceived gaze direction: Linear combination of eye and head cues

Yumiko Otsuka

University of New South Wales, Kensington,  
New South Wales, Australia  
Ehime University, Matsuyama, Ehime, Japan



Isabelle Mareschal

Queen Mary University of London, England



Colin W. G. Clifford

University of New South Wales, Kensington,  
New South Wales, Australia



We have recently proposed a dual-route model of the effect of head orientation on perceived gaze direction (Otsuka, Mareschal, Calder, & Clifford, 2014; Otsuka, Mareschal, & Clifford, 2015), which computes perceived gaze direction as a linear combination of eye orientation and head orientation. By parametrically manipulating eye orientation and head orientation, we tested the adequacy of a linear model to account for the effect of horizontal head orientation on perceived direction of gaze. Here, participants adjusted an on-screen pointer toward the perceived gaze direction in two image conditions: Normal condition and Wollaston condition. Images in the Normal condition included a change in the visible part of the eye along with the change in head orientation, while images in the Wollaston condition were manipulated to have identical eye regions across head orientations. Multiple regression analysis with explanatory variables of eye orientation and head orientation revealed that linear models account for most of the variance both in the Normal condition and in the Wollaston condition. Further, we found no evidence that the model with a nonlinear term explains significantly more variance. Thus, the current study supports the dual-route model that computes the perceived gaze direction as a linear combination of eye orientation and head orientation.

Todorovic, 2006, 2009; Wollaston, 1824, and in the periphery, Florey, Dakin, Clifford, & Mareschal, 2015). Under normal three-dimensional (3D) conditions, a repulsive effect of head orientation is generally observed (Anstis et al., 1969; Gamer & Hecht, 2007; Gibson & Pick, 1963; Masame, 1990; Noll, 1976; Otsuka et al., 2014; Otsuka et al., 2015). When facial images are manipulated two-dimensionally so that identical eyes are placed in a different facial orientation context, as in the demonstration by Wollaston (1824), an attractive effect is observed (Langton et al., 2004; Maruyama & Endo, 1983; Todorovic, 2006, 2009). Recently, we have proposed a dual-route model (see Figure 1) to provide a quantitative account of the influence of head orientation on gaze perception (Otsuka et al., 2014; Otsuka et al., 2015).

The dual-route model computes perceived gaze direction as a linear combination of eye orientation and head orientation. A schematic of the dual-route model describing how eye orientation and head orientation jointly influence perceived gaze direction is shown in Figure 1. In the normal 3D situation (Figure 1A), the effect of head turn involves two distinct routes, corresponding to the two arrows from head orientation. First, the route that induces the repulsive effect is illustrated as the arrow from head orientation to eye-region information, suggesting that head orientation acts as an indirect cue for the perceived gaze direction via the change in eye-region of the proximal stimulus. This effect occurs because turning the head induces a shift of the relative position of the iris within the eyes (Anstis et al., 1969). Figure 2A (Normal) illustrates the effect of head turn on the eye-region information that can occur even when eye orientation is fixed ( $0^\circ$  to the observer in this example). The images of the eye-region

## Introduction

Numerous previous studies have shown that head orientation has a significant influence on the perceived gaze direction (e.g., Anstis, Mayhew, & Morley, 1969; Gamer & Hecht, 2007; Gibson & Pick, 1963; Langton, 2000; Langton, Honeyman, & Tessler, 2004; Ricciardelli & Driver, 2008; Seyama & Nagayama, 2005;

Citation: Otsuka, Y., Mareschal, I., & Clifford, C. W. G. (2016). Testing the dual-route model of perceived gaze direction: Linear combination of eye and head cues. *Journal of Vision*, 16(8):8, 1–12, doi:10.1167/16.8.8.

doi: 10.1167/16.8.8

Received September 30, 2015; published June 9, 2016

ISSN 1534-7362



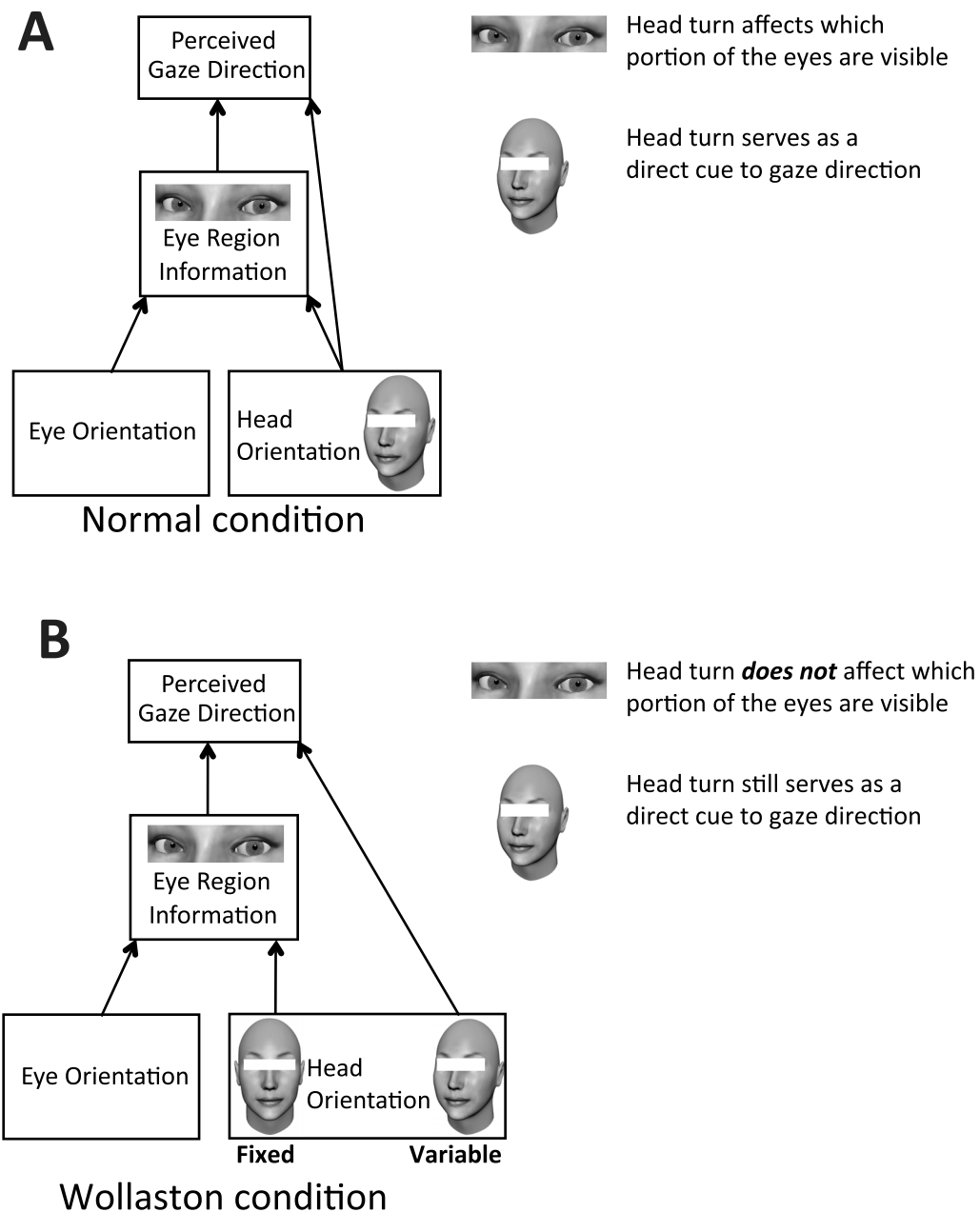


Figure 1. Schematic of the dual-route model (Otsuka et al., 2014) as applied to the Normal condition and the Wollaston condition. These schemes describe how stimulus eye orientation and head orientation jointly influence perceived gaze direction in the situation that observers have to infer the gaze direction of a stimulus with particular eye orientation and head orientation. Note that the boxes labeled as eye orientation and head orientation at the outset of the schemes in no way mean that observers have direct access to this information. Rather, observers base their decision on eye region information and head orientation in the proximal stimulus. (A) The influence of head turn normally involves two distinct routes: as an indirect cue via the change in eye-region information, and as a direct cue via head orientation. (B) As the Wollaston images have identical eye-regions from a forward-facing head, the influence of head turn in the Wollaston condition is limited to the direct cue only.

under each of the faces are magnified parts of the eye-region of each face. The images of the eyeballs under the eye-region images in Figure 2A (Normal) depict the eyeballs located behind the eye openings for each of the eye-region images. The eyeball images illustrate that the eyeballs are oriented straight ahead toward the observer ( $0^\circ$ ) regardless of the head orientation.

However, observers do not have access to the full view of the eyeballs in the eye-region of faces. When observers have to infer the gaze direction from faces, therefore, their perception of gaze direction is affected by the portion of the visible eye area. This is why the eye-regions in Figure 2A (Normal) appear to have different eye orientations (gaze direction biased oppo-

site to head orientation: repulsive, indirect effect of head orientation) although the eyeball orientation is the same.

Second, information about head orientation acts as a direct cue for gaze direction that attracts the perceived gaze direction toward the head orientation (attractive effect) and thus tends to compensate for the bias occurring through the former effect. This latter route of the effect of head orientation is illustrated by the direct arrow from head orientation to perceived gaze direction in the schematic (Figure 1A). The direct effect is illustrated in the Figure 2A (Wollaston). Based on the demonstration by Wollaston (1824), we created Wollaston images by taking the part of the 0° head orientation image corresponding to the eye-region, and two-dimensionally superimposed it onto faces with various head orientations. Thus, the eye-region was identical across head orientations in the Wollaston images (see the magnified parts of the eye-region for each of the Wollaston faces in Figure 2A). Nevertheless, the faces in the Wollaston images appear to be gazing at different directions. We think this is because head orientation acts directly as a cue to gaze direction, which attracts the perceived gaze direction toward the head orientation.

In the normal 3D situation, which involves both routes whereby head turn affects perceived gaze direction (Figure 1A), the repulsive effect is compensated by the simultaneously occurring attractive effect. As the compensation by attractive effect is imperfect, an overall repulsive effect of head orientation is generally observed (Anstis et al., 1969; Gamer & Hecht, 2007; Gibson & Pick, 1963; Masame, 1990; Noll, 1976). The indirect effect of head orientation on the eye region operates even when the head itself is not visible via the change in the eye-region information. As illustrated in the eye-region images of Figure 2A (Normal), when little information about head orientation is available, thereby reducing the attractive effect that otherwise serves to counteract the indirect effect, such a repulsive effect becomes most pronounced (Otsuka et al., 2014; Otsuka et al., 2015). When facial images are manipulated two-dimensionally so that an identical eye-region is placed in a differential facial orientation context, as in the demonstration by Wollaston (1824, see also Figure 2A Wollaston), the influence of the indirect cue is eliminated. As the influence of head turn in such a condition involves only a direct cue (Figure 1B), an attractive effect is observed (Langton et al., 2004; Maruyama & Endo, 1983; Todorovic, 2006, 2009). Note that the difference in how the dual-route model is applied in Figure 1A and 1B reflects only the difference in the *stimulus* between the two conditions. In this way, the dual-route model provides a framework to understand the relationship between the two opposing effects

of head orientation on perceived gaze direction identified in the previous studies.

While the dual-route model computes perceived gaze direction as a linear combination of eye orientation and head orientation, some of the previous studies suggested a nonlinear combination of these cues (Cline, 1967; Gonzalez-Franco & Chou, 2014). For example, Cline (1967) reported that the gaze estimation error was reduced when the eye orientation and head orientation were aligned. More recently, Gonzalez-Franco and Chou (2014) reported that the perception of horizontal gaze direction as measured in their study was best described by a nonlinear combination of these cues.

The current study tested the dual-route model by examining whether a linear combination between eye orientation and head orientation is sufficient to account for the perceived gaze direction, or whether a nonlinear term is in fact necessary. We measured the perceived gaze direction for various horizontal eye orientations in the context of various head orientations by means of an on-screen pointer as used by Mareschal, Otsuka, and Clifford (2014, see Figure 2C). Further, we parametrically manipulated stimulus eye orientation between  $\pm 20^\circ$  and stimulus head orientation between  $\pm 25^\circ$  in steps of  $5^\circ$  each. This allowed us to test the adequacy of a linear model (Otsuka et al., 2014; Otsuka et al., 2015) to capture the effect of horizontal head orientation on perceived direction of gaze. The perceived gaze direction was measured in two stimulus conditions: the Normal condition and the Wollaston condition. Each image in the Normal condition contained a change in the eye-region that was consistent with the head orientation change in three dimensions (see Figure 2A Normal). Conversely, in the Wollaston condition, the eye-region from a directly facing head was superimposed onto an angled face (Figure 2A Wollaston), removing the change in the eye-region that would normally accompany the head orientation change. Therefore, the Wollaston condition involved only the influence of head turn as a direct cue, whereas the normal condition involved both direct and indirect effects of head turn (see Figure 1).

## Experiment

### Methods

#### Participants

Sixteen naïve observers (eight male and eight female) served as subjects for both the Normal (mean age = 25.3 years) and Wollaston conditions (mean age = 21.9 years). Additionally, one of the authors (CC) and seven naïve observers served as subjects in the Control experiment (mean age = 25.8 years). One additional

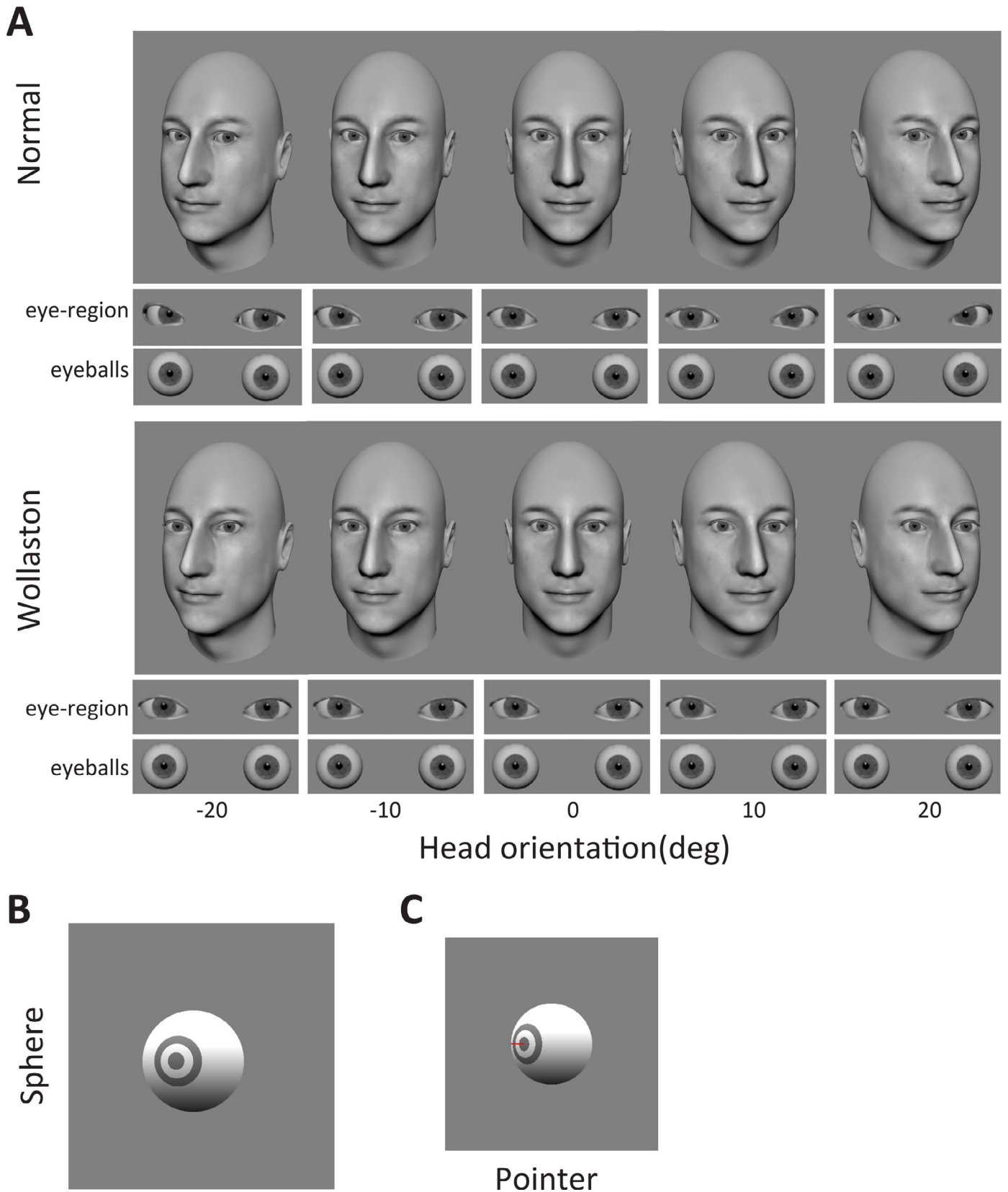


Figure 2. Example of stimuli and procedure. (A) Example of synthetic faces with eye orientation of  $0^\circ$  in various head orientations in the Normal and the Wollaston conditions. The images of the eye-region under each of the faces are magnified parts of the eye-region of each face. The images of the eyeballs under each eye-region illustrate the constant eyeball orientation behind the eye openings for

→

←

each eye-region image. (B) Example of a sphere image oriented  $-20^\circ$ , as shown in the Control condition. (C) Example image of on-screen pointer used to indicate the perceived gaze direction (or the sphere orientation in the Control condition). On each trial, the pointer appeared at the center of the screen immediately after the face stimulus disappeared.

observer was tested in the Wollaston condition but excluded from analysis, because it was apparent from the data that this subject misunderstood the task and adjusted the pointer toward the orientation of the heads. All subjects had normal or corrected to normal vision. All experiments adhered to the declaration of Helsinki guidelines and were approved by the University of New South Wales Human Research Ethics Committee.

### Apparatus

A computer running Matlab™ (MathWorks, Natick, MA) was used for stimulus generation, experiment control, and recording subjects' responses. The programs controlling the experiment incorporated elements of the PsychToolbox (Brainard, 1997). Stimuli were displayed on a Viewsonic Graphics Series G90f CRT monitor (ViewSonic, Brea, CA) ( $1024 \times 768$  pixels). At the viewing distance of 57 cm, one pixel subtended 2 arcmin.

### Stimuli

Examples of the stimuli are shown in Figure 2. Four gray-scale synthetic neutral faces (two male and two female faces) were created using FaceGen Modeller 3.5 (Singular Inversions, Toronto, Canada). The 3D models of the faces created in FaceGen were imported into Blender 2.70. The original eyes in the faces were replaced with 3D model eyes created in Blender. Each eye was set to track a fixation target using the "AutoTrack" feature in Blender. The orientation of each eye was controlled by changing the angular position of the fixation target in the horizontal plane. Images for the Normal condition were the ones originally rendered in Blender. The images for the Wollaston condition were created by inserting the eye-region of the frontal face ( $0^\circ$  pose) into each of the angled faces (11 angles). This was done by superimposing the eye-region of the frontal face image upon that of the angled face using Photoshop (Adobe, San Jose, CA). The surrounding area of the eye-region was retouched so that it merged well with the skin on each of the new faces, but the eye-region including the edges of the eyelids were identical across the head orientations. Thus, the stimuli were identical only for the  $0^\circ$  head orientation between the Normal and the Wollaston condition. Other than the case of the  $0^\circ$  head orientation, the stimulus images differed between the Normal and the Wollaston conditions. In addition to

the difference in the relative position of the iris within the eyes, factors such as the shape of the eye-opening differed between the two conditions because only the eye-region in the Normal condition was affected by foreshortening. These differences were more pronounced for faces with greater head angle (compare Figure 2A eye-region images in the two conditions). All face images were rendered with the camera pointed at the right eye of each face, as this setting ensured the optimal fitting of the eyes of the frontal faces into the angled faces without any rotation of the eyes or change in the distance between the eyes. A single light source from above the camera illuminated the faces. To avoid introducing any horizontal bias during stimulus production, we used left-right reversed versions of the originally created images for half of the facial identities in each condition. All images were shown against a medium gray background ( $18.25\text{cd/m}^2$ ). The faces subtended about  $24^\circ \times 14^\circ$  of visual angle and were viewed at 57 cm in a dimly lit room.

An on-screen pointer (Figure 2C) consisting of a sphere and a red extender line was rendered and controlled using Matlab. The spherical part of the pointer subtended 5.07 degrees of visual angle (148 pixels) in diameter, and its angle could vary  $180^\circ$  in the horizontal plane according to the x location of a computer mouse. The projected length of the red extender line also indicated the magnitude of the angle. In addition, the sphere images for the Control condition consisting of the spherical part of the pointer in a larger size ( $10.14^\circ$  of visual angle in diameter) were rendered using Matlab.

### Procedure

The observers' task was to indicate the perceived direction of gaze by adjusting the on-screen pointer that appeared following the face stimulus. Each face stimulus was presented in a raised cosine temporal window, such that ramping on and off took 250 ms each (total duration of 500 ms), followed immediately by the presentation of the pointer. On each trial, the position of the face stimulus was randomly jittered horizontally and vertically within  $\pm 0.83^\circ$  of visual angle around the center of the screen. Following the disappearance of the face stimulus, the pointer appeared at the center of the screen. The pointer remained visible until the observer terminated the trial by clicking the mouse button after adjusting the horizontal angle of the pointer with the mouse. The initial horizontal angle of the pointer was randomly set in the range  $\pm 90^\circ$  on each trial. The vertical

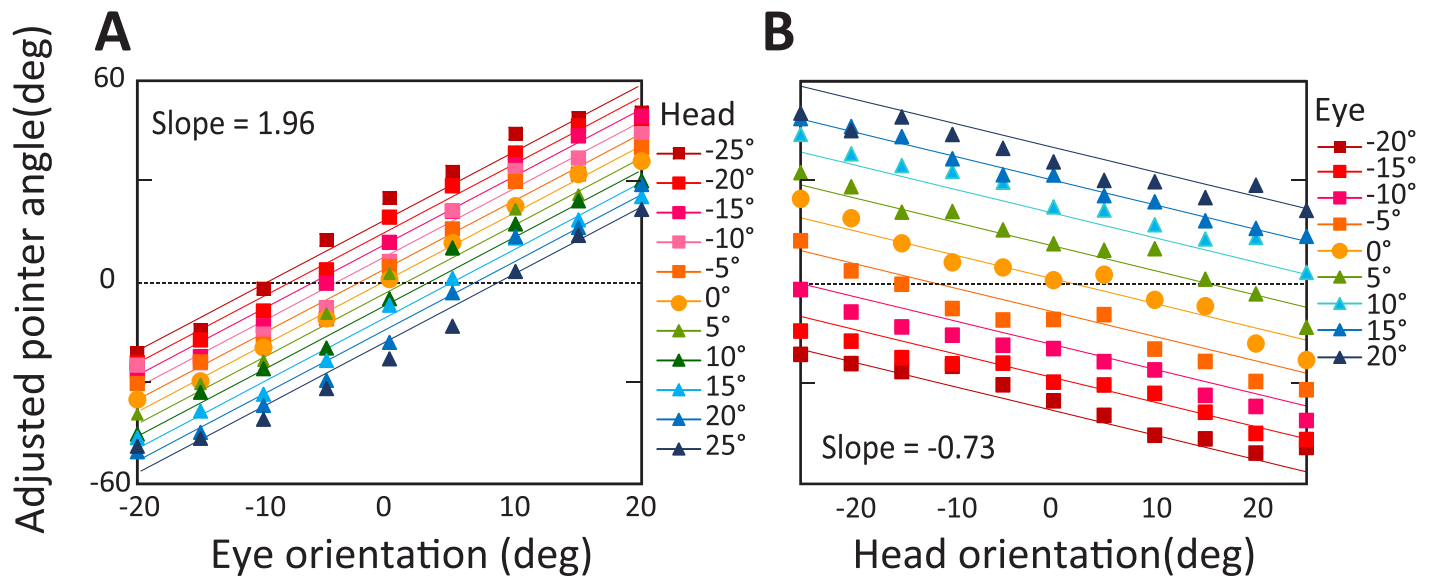


Figure 3. Data from the Normal condition averaged across subjects ( $n = 16$ ). (A) Averaged adjusted pointer angle as a function of eye orientation for each head orientation together with the linear fits. (B) Averaged adjusted pointer angle as a function of head orientation for each eye orientation together with the linear fits.

angle of the pointer was fixed to  $0^\circ$ . After each response, the next trial was initiated following a 600 ms wait period with a blank gray screen.

Participants were randomly assigned to one of the conditions, and were not aware of the stimulus manipulation in either of the conditions. In the Normal and Wollaston conditions, each participant completed a total of 396 trials consisting of four blocks of 99 trials. Across the four blocks, stimuli were presented in a random order with 4 facial identity (two male and two female)  $\times$  11 head orientation  $\{-25^\circ, -20^\circ, -15^\circ, -10^\circ, -5^\circ, 0^\circ, 5^\circ, 10^\circ, 15^\circ, 20^\circ, 25^\circ\}$   $\times$  9 eye orientation  $\{-20^\circ, -15^\circ, -10^\circ, -5^\circ, 0^\circ, 5^\circ, 10^\circ, 15^\circ, 20^\circ\}$ . Note that we use the term “eye orientation” to refer to the physical orientation of the eyes relative to the observer. We reserve the term “gaze direction” for the subjective percept. In the Control condition, subjects performed two blocks of 36 trials either consisting of frontal face presentation (4 facial identity  $\times$  9 eye orientation in  $0^\circ$  head orientation) or of sphere presentation (9 sphere orientation  $\times$  4 repeat).

## Results and discussion

The results from the Normal condition are summarized in Figure 3. Figure 3A shows the averaged adjusted pointer angle as a function of eye orientation for each head orientation in the Normal condition. The adjusted pointer angle tends to increase monotonically as the eye orientation is varied from left to right, with a slight tendency for responses to saturate at extreme eye orientation. Further, there is a clear

decrease in the adjusted pointer angle as the head orientation is varied from leftward ( $-25^\circ$ ) to rightward ( $25^\circ$ ). This shift is of consistent magnitude across eye orientations, suggesting that the effect of head orientation on the perceived gaze direction is constant across eye orientations. Figure 3B shows the same data plotted as a function of head orientation for each eye orientation. This plot shows a clear trend for the adjusted pointer angle for each eye orientation to decrease monotonically as the head orientation is varied from left to right, suggesting that the perceived gaze direction is biased opposite to the head orientation (repulsive effect).

We performed multiple regression analysis on the mean adjusted pointer angle across subjects with explanatory variables of eye orientation and head orientation.

The resulting equation was:

$$\text{Pointer angle} = 0.82 + 1.96 \times \text{eyes} - 0.73 \times \text{head} - 0.0004 \times (\text{eyes} \times \text{head})$$

Note that the negative value attached to head orientation here suggests that the perceived gaze direction is biased opposite to the head orientation (repulsive effect). We followed Dobson (1990) in using an  $F$  test to establish whether a linear model (Pointer angle =  $0.82 + 1.96 \times \text{eyes} - 0.73 \times \text{head}$ ) is sufficient to account for the perceived gaze direction, or whether the nonlinear (eyes  $\times$  head) term is in fact necessary. The fit of the model with the additional nonlinear term is inevitably better than for the linear model. Thus, the introduction of the additional parameter is justified only if the fit of the more complex model is significantly

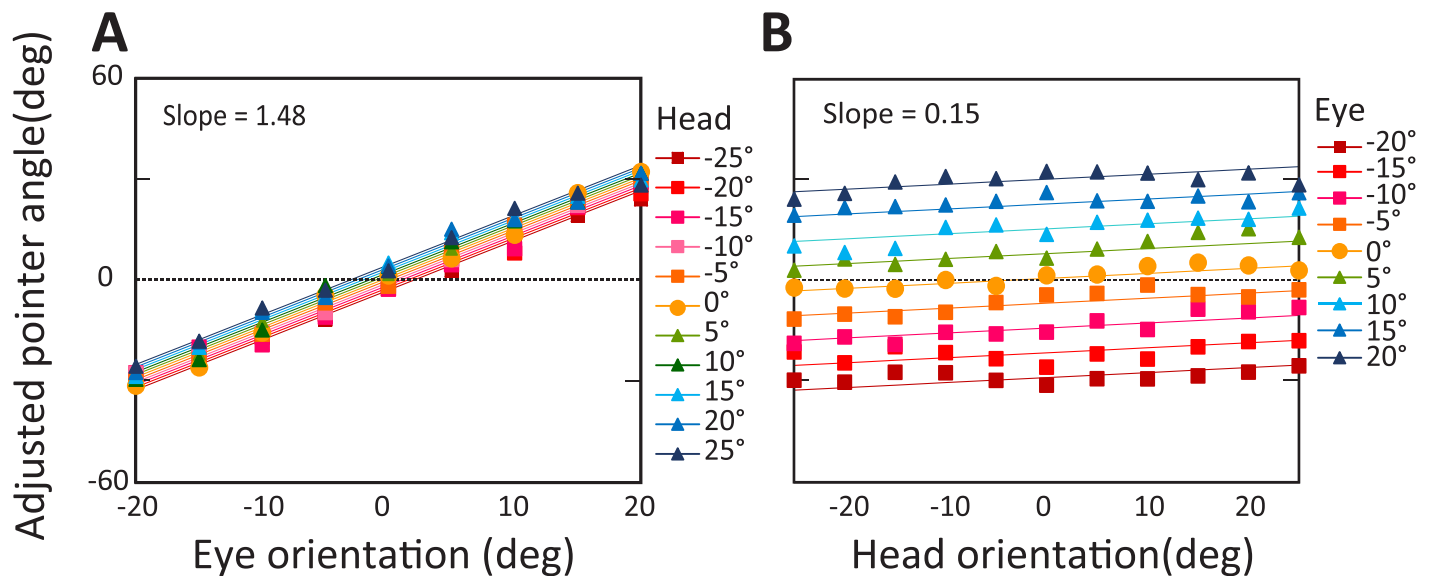


Figure 4. Data from the Wollaston condition averaged across subjects ( $n = 16$ ). (A) Averaged adjusted pointer angle as a function of eye orientation for each head orientation together with the linear fits. (B) Averaged adjusted pointer angle as a function of head orientation for each eye orientation together with the linear fits.

better than that of simple one. The percentage of variance explained by the model with linear combination between eye orientation and head orientation was 98.3%. Comparison of residual errors showed that the fit of the model with a nonlinear term does not explain significantly more variance,  $F(1, 96) = 0.05$ ,  $p = 0.82$ . Thus, the linear model without a nonlinear term is preferred.

The linear fits to the initial data plots as a function of eye orientation are shown in Figure 3A. The slope of the regression line was 1.96 (95% CI = 1.73, 2.22), showing that the eye orientation was largely overestimated (confidence intervals throughout are obtained by bootstrapped resampling across subjects). The linear fits to the initial data plots as a function of head orientation are shown in Figure 3B. The slope of the regression line was  $-0.73$  (95% CI =  $-0.97$ ,  $-0.5$ ). The negative slope shows a repulsive effect of head orientation on the perceived gaze direction.

The results from the Wollaston condition are summarized in Figure 4. Figure 4A shows the averaged adjusted pointer angle as a function of eye orientation for each head orientation pose in the Wollaston condition. Again, the adjusted pointer angle tends to increase monotonically as the eye orientation is varied from left to right. Unlike in the Normal condition, the adjusted pointer angle tends to *increase* slightly as head orientation is varied from leftward to rightward. This tendency is consistent across eye orientation. Figure 4B shows the same data plotted as a function of head orientation for each eye orientation.

We performed multiple regression analysis on the mean adjusted pointer angle across subjects with

explanatory variables of eye orientation and head orientation. The resulting equation was:

$$\text{Pointer angle} = 0.75 + 1.48 \times \text{eyes} + 0.15 \times \text{head} - 0.0011 \times (\text{eyes} \times \text{head})$$

The percentage of variance explained by the linear model (Pointer angle =  $0.75 + 1.48 \times \text{eyes} + 0.15 \times \text{head}$ ) was 98.9%. As in the Normal condition, comparison of residual errors show that the fit of the model with a non-linear term (eyes  $\times$  head) does not explain significantly more variance,  $F(1, 96) = 1.15$ ,  $p = 0.29$ . Thus, the linear model without a nonlinear term is preferred.

The linear fits to the initial data plots as a function of eye orientation are shown in Figure 4A. The slope of the regression line was 1.48 (95% CI = 1.27, 1.71), showing that the eye orientation was overestimated as in the Normal condition. The linear fits to the initial data plots as a function of head orientation are shown in Figure 4B. The slope of the regression line was 0.15 (95% CI =  $-0.01$ , 0.29). The positive slope shows that the perceived gaze direction was attracted toward the head orientation (attractive effect).

In a Control experiment, we tested a smaller number of subjects using frontal face images and sphere images to see whether the over estimation of orientation is unique to the judgment of gaze direction. The results from the Control experiment are summarized in Figure 5. Figure 5 shows the averaged adjusted pointer angle as a function of eye orientation (Frontal condition) or as a function of sphere orientation (Sphere condition) together with the linear fits. The slope of the regression line for the Frontal



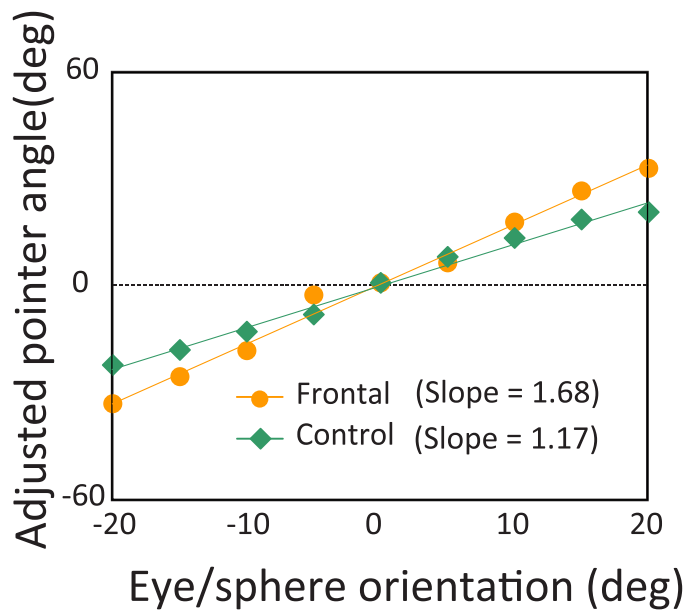


Figure 5. Data from the Control experiment averaged across subjects ( $n = 8$ ). (A) Averaged adjusted pointer angle as a function of eye/sphere orientation in the Frontal condition and in the Sphere condition, together with the linear fits.

condition was 1.68 (95% CI = 1.41, 1.93), showing a large overestimation of gaze direction as found in the Normal and Wollaston conditions. The slope of the regression line for the Sphere condition was 1.17 (95% CI = 1.07, 1.30). That the slope of the regression line is greater than 1 shows that there was a slight overestimation even for the Sphere condition, although the slope was significantly shallower than for the Frontal condition ( $p < 0.01$ ), as established by bootstrapped resampling across subjects.

## General discussion

By parametrically manipulating eye orientation and head orientation, we tested the adequacy of a linear model (Otsuka et al., 2014, 2015) to capture the effect of horizontal head orientation on perceived direction of gaze. We found that a linear model accounts well for the perceived gaze direction with 98.3% of variance explained in the Normal condition and 98.9% in the Wollaston condition. Further, we found no evidence that adding an interaction term in combining eye and head cues significantly improves the fit. Thus, the current results support the validity of the dual-route model in computing the perceived gaze direction as a linear combination of eye orientation and head orientation.

The nonlinear combination of head and eye cues was suggested by Cline (1967) and Gonzalez-Franco and

Chou (2014). Cline reported that his subjects showed a smaller bias in the perceived gaze direction when the looker's head and gaze were aligned compared with when they were misaligned. We note that the linear regression model from the Normal condition in the current study predicts such a pattern of results among the combinations of eye orientation and head orientation tested by Cline ( $0^\circ, \pm 4^\circ, \pm 10^\circ$  eye orientation with  $0^\circ$  and  $30^\circ$  head orientation, and  $0^\circ, \pm 4^\circ, \pm 10^\circ$  aligned head and eye angle). However, across the more comprehensive range of eye and head orientations we tested in the current study ( $\pm 20^\circ$ ), the model does not predict that bias is smallest when the eye orientation and head orientation are aligned. Thus, the dual-route model can account for results of Cline, but our results do not support the generality of the notion of reduced bias when the eye orientation and head orientation are aligned. Although Gonzalez-Franco and Chou reported that perception of horizontal gaze direction is best described by a nonlinear combination of these cues, the variance accounted for with their nonlinear model reported in their study is smaller than what was found in the current study. Thus, the simpler linear model proposed here is preferable. We also note that Gonzalez-Franco and Chou gave feedback after each trial as to the veridical orientation of gaze. We are concerned that this complicates interpretation of their data as subjects likely tried to correct for their intrinsic perceptual biases during the course of the experiment.

We found that subjects consistently overestimate eye orientation. The slopes as a function of eye orientation are between 1.48 and 1.96 (Figure 3A, Figure 4A, Figure 5 frontal condition), meaning that, for example, a  $20^\circ$  eye orientation would typically lead to a roughly  $35^\circ$  pointer setting. Overestimation of eye orientation is consistent with findings from several previous studies. Previous studies that fitted regression lines to the judged gaze direction as a function of actual eye orientation have consistently reported the slope to be greater than 1 (Anstis et al., 1969: between 1.50 to 1.82; Imai, Sekiguchi, Inami, Kawakami, & Tachi, 2006: 1.16 to 1.21; Masame, 1990: 1.05; Todorovic, 2009: 1.35, note images used in Todorovic study were schematic faces).

Previous studies have reported a tendency for the perceived direction of another's gaze to be biased towards the observer (i.e.,  $0^\circ$  eye orientation) under conditions of uncertainty, such as when the eye region is indistinct (Mareschal, Calder, & Clifford, 2013; Mareschal et al., 2014; Martin & Rovira, 1981). As mentioned previously, however, the current study and several previous studies (e.g., Anstis et al., 1969) have shown that, when the eye-region is clearly visible, the orientation of eyes from direct is *over*-estimated. How can these observations be reconciled? This question prompted us to reexamine the data that we published in

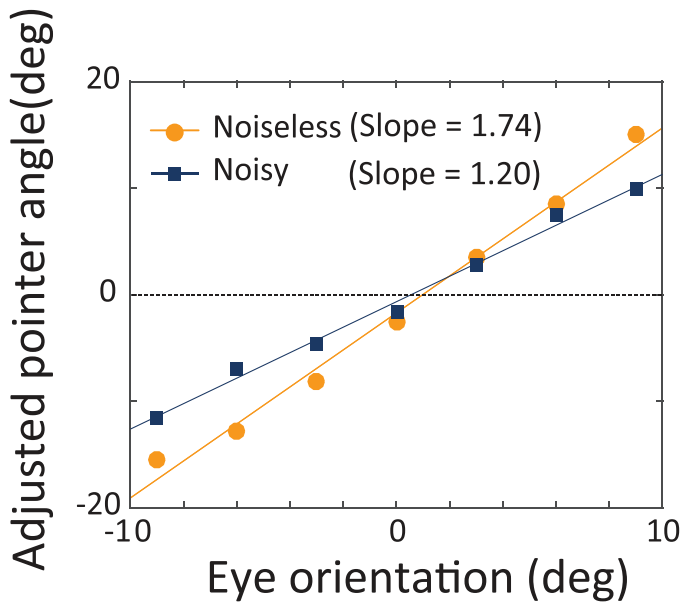


Figure 6. Reanalysis of data from Mareschal et al. (2014). Adjusted pointer angle for the Noiseless and Noisy condition as a function of the horizontal eye orientations with frontal face together with the linear fits.

Mareschal et al. (2014) comparing perceived gaze direction in noiseless and noisy conditions for horizontal eye orientations with a direct head. In the noiseless condition, the eyes were presented at high contrast, as in the current study. In the noisy condition, pupil-sclera contrast was reduced and spatial noise was added, manipulations that together degraded the information available from the eye region. The range of eye orientations tested in that study was only  $\pm 9^\circ$ , as opposed to  $\pm 20^\circ$  here; nonetheless, a similar overestimation of the orientation of the eyes from direct gaze is evident in the noiseless condition (Figure 6, orange line). This overestimation is reduced in the noisy condition (Figure 6, blue line) to a level similar to the control condition in the current study. Thus, it appears that in noiseless conditions there is a consistent bias to overestimate the orientation of the eyes from direct and that, under conditions of uncertainty, a prior expectation for gaze to be directed at the observer tends to reduce, but not reverse, this effect.

Interestingly, an analogous pattern of bias has been reported in the domain of orientation perception (Tomassini, Morgan, & Solomon, 2010). In noiseless conditions, there is a bias for orientations to be reported as more oblique (i.e., less horizontal/vertical) than they really are. However, this effect has been reported to decrease but not reverse with uncertainty (Tomassini et al., 2010), consistent with a prior for cardinal (horizontal/vertical) orientations (Girshick, Landy, & Simoncelli, 2011; Wei & Stocker, 2015). This leads to the counterintuitive observation that the perception of orientation (and gaze direction) is

actually closer to veridical (i.e., more accurate, though, of course, less precise) under conditions of uncertainty, as though our perception is somehow “optimized” to operate in conditions of uncertainty.

We used the weights of the linear regression model in the Normal condition and the Wollaston condition to infer the weighting on the direct cue and indirect cue of head orientation in the dual-route model. The dual-route model computes the perceived direction of gaze,  $G$ , as a weighted average of the eye orientation,  $E$ , and head orientation,  $H$ , such that two weights are constrained to sum to one (Figure 7).

Thus, for the Normal condition (Figure 7B) we can model the perceived direction of gaze,  $G_{\text{NORMAL}}$ , as:

$$G_{\text{NORMAL}} = \beta E + (1 - \beta)H \quad (1)$$

In the Normal condition, the weighting,  $(1 - \beta)$ , attached to head orientation reflects the aggregate effect of head orientation on eye region information [indirect cue: modeled as  $(1 - \alpha)$ ] and as an explicit cue to gaze direction in its own right [direct cue: modelled as  $1 - (\beta / \alpha)$ ]. Decomposing the influence of head orientation into direct and indirect cues (Figure 7A), we expand Equation 1 to give:

$$G_{\text{NORMAL}} = \frac{\beta}{\alpha} (aE + (1 - \alpha)H) + H \left(1 - \frac{\beta}{\alpha}\right) \quad (2)$$

For the Wollaston condition, identical eye-regions are inserted into the different head orientation contexts. Thus, all of the eye-region information comes from eye direction and we can model the perceived direction of gaze,  $G_{\text{WOLLASTON}}$ , as:

$$G_{\text{WOLLASTON}} = \frac{\beta}{\alpha} E + H \left(1 - \frac{\beta}{\alpha}\right) \quad (3)$$

The fits of the regression models give the relative weighting of the eye and head cues in the Normal and Wollaston conditions. These we term  $m_{\text{Normal}}^{\text{Eye}}$ ,  $m_{\text{Normal}}^{\text{Head}}$ ,  $m_{\text{Wollaston}}^{\text{Eye}}$ , and  $m_{\text{Wollaston}}^{\text{Head}}$ , respectively. Applying the constraint that in the dual-route mode the weights on eye and head in each condition sum to one gives us, for the Normal condition (Equation 1):

$$\beta = \frac{m_{\text{Normal}}^{\text{Eye}}}{m_{\text{Normal}}^{\text{Eye}} + m_{\text{Normal}}^{\text{Head}}} \quad (4)$$

and for the Wollaston condition (Equation 2):

$$\frac{\beta}{\alpha} = \frac{m_{\text{Wollaston}}^{\text{Eye}}}{m_{\text{Wollaston}}^{\text{Eye}} + m_{\text{Wollaston}}^{\text{Head}}} \quad (5)$$

Solving Equations 4 and 5 for  $\alpha$  gives:

$$\alpha = \left( \frac{m_{\text{Wollaston}}^{\text{Eye}} + m_{\text{Wollaston}}^{\text{Head}}}{m_{\text{Normal}}^{\text{Eye}} + m_{\text{Normal}}^{\text{Head}}} \right) \cdot \left( \frac{m_{\text{Normal}}^{\text{Eye}}}{m_{\text{Normal}}^{\text{Head}}} \right) \quad (6)$$

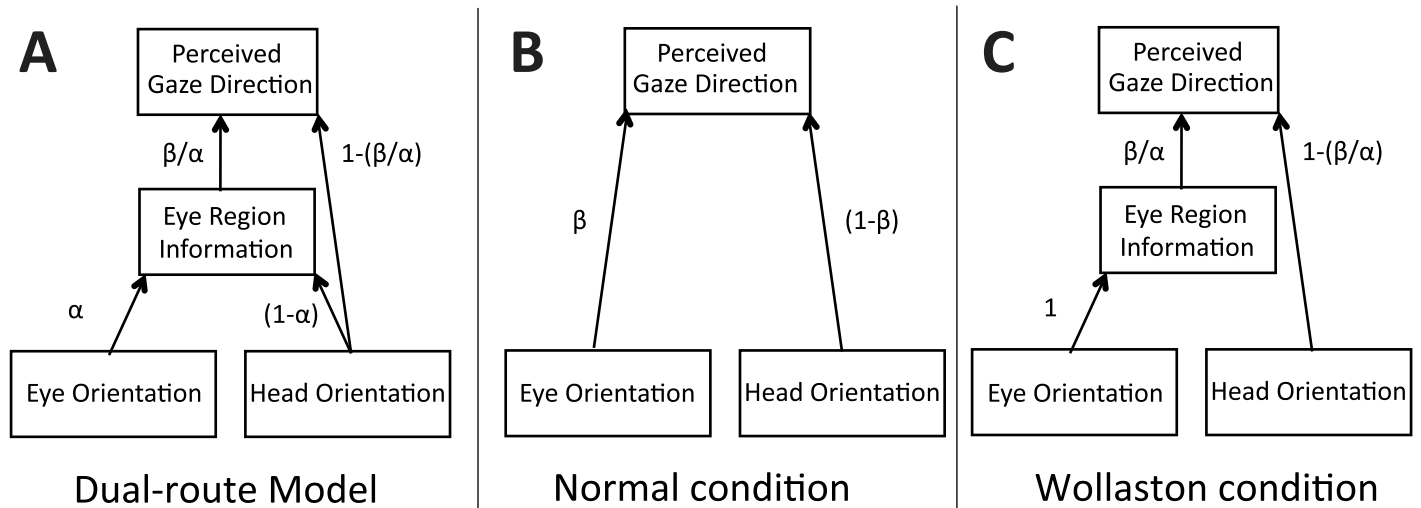


Figure 7. Illustration of the functional significance of the weights  $\alpha$  and  $\beta$  in the context of the dual-route model (Otsuka et al., 2014) as applied to the Normal (A and B) and Wollaston conditions (C). Specifically,  $\beta$  represents the weight attached to eye direction in the Normal condition, while  $\alpha$  represents the contribution of eye direction in the Wollaston condition.

Figure 8 shows the dual-route model with the weight attached to each cue calculated based on the current results. While the positive weight attached to the direct cue and negative weight attached to indirect cue shows qualitative agreement, there is some qualitative difference between the current study and our previous study. The weight attached to the direct cue is 0.09, which is similar to the corresponding weight of 0.13 in our previous studies (Otsuka et al., 2014; 2015). On the other hand, the weight attached to the indirect cue is  $-0.75$ , which is considerably larger than the corresponding weight of  $-0.27$  to  $-0.39$  in our previous studies (Otsuka et al., 2014; Otsuka et al., 2015).

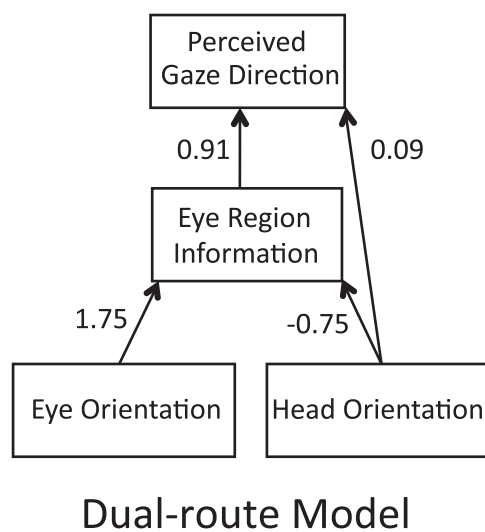


Figure 8. Dual-route model for the influence of head orientation on perceived gaze direction. The weights attached to each cue were derived by comparing the experimental results from the Normal and Wollaston conditions.

We recently introduced the idea of a gaze constancy index to quantify the degree to which perceived gaze direction is robust to changes in head orientation (Otsuka et al., 2015). If subjects were completely unable to discount the effect of head orientation on eye region information and simply used the direction of the eye relative to the head to estimate gaze direction (i.e., a gaze constancy index of 0) then the value of the weight attached to the indirect cue of head orientation would be  $-1$ . If, instead, subjects were able to make perfect use of information from the eye region (i.e., a gaze constancy index of 1), such as the projected shape of the eye, to discount the effect of head orientation then the value of the weight attached to the indirect cue of head orientation would be zero. The weight of  $-0.75$  on the indirect cue inferred from current data corresponds to a gaze constancy index of 0.25, rather poorer than the index of 0.8 we reported previously (Otsuka et al., 2015).

We are currently unsure as to what can explain the difference between studies in the magnitude of the weight attached to the indirect cue and consequent estimates of the value of the gaze constancy index. Given the generation of stimuli and the image presentation procedure used in the current study is closer to one of our previous studies (Otsuka et al., 2015) than the other study (Otsuka et al., 2014), stimulus properties are unlikely to explain the deviant results found in the current study. More importantly, the current study asked subjects to adjust the angle of the on-screen pointer toward the perceived gaze direction, while our previous studies employed a gaze categorization task. The current task revealed overestimation of eye orientation, which cannot be revealed by the categorization task. Considering that in the



- The influence of head contour and nose angle on the perception of eye-gaze direction. *Perception & Psychophysics*, 66(5), 752–771, doi:10.3758/BF03194970.
- Mareschal, I., Calder, A. J., & Clifford, C. W. G. (2013). Humans have an expectation that gaze is directed towards them. *Current Biology*, 23, 717–721, doi:10.1016/j.cub.2013.
- Mareschal, I., Otsuka, Y., & Clifford, C. W. (2014). A generalized tendency toward direct gaze with uncertainty. *Journal of Vision*, 14(12):27, 1–9, doi:10.1167/14.12.27. [PubMed] [Article]
- Martin, W. W., & Rovira, L. M. (1981). An experimental analysis of discriminability and bias in eyegaze judgment. *Journal of Nonverbal Behaviour*, 5(3), 155–163.
- Maruyama, K., & Endo, M. (1983). The effect of face orientation upon apparent direction of gaze. *Tohoku Psychologica Folia*, 42, 126–138.
- Masame, K. (1990). Perception of where a person is looking: Overestimation and underestimation of gaze direction. *Tohoku Psychologica Folia*, 49, 33–41.
- Noll, A. M. (1976). The effects of visible eye and head turn on the perception of being looked at. *The American Journal of Psychology*, 89(4), 631–644.
- Otsuka, Y., Mareschal, I., Calder, A., and Clifford, C. W. G. (2014). Dual-route model of the effect of head orientation on perceived gaze direction. *Journal of Experimental Psychology: Human Perception & Performance*, 40(4), 1425–1439, doi:10.1037/a0036151.
- Otsuka, Y., Mareschal, I., & Clifford, C. W. G. (2015). Gaze constancy in upright and inverted faces. *Journal of Vision*, 15(1):21, 1–14, doi:10.1167/15.1.21. [PubMed] [Article]
- Ricciardelli, P., & Driver, J. (2008). Effects of head orientation on gaze perception: How positive congruency effects can be reversed. *Quarterly Journal of Experimental Psychology*, 61, 491–504, doi:10.1080/17470210701255457.
- Seyama, J., & Nagayama, R. (2005). The effect of torso direction on the judgement of eye direction. *Visual Cognition*, 12, 103–116, doi:10.1080/13506280444000111.
- Todorovic, D. (2006). Geometrical basis of perception of gaze direction. *Vision Research*, 46(21), 3549–3562, doi:10.1016/j.visres.2006.04.011.
- Todorovic, D. (2009). The effect of face eccentricity on the perception of gaze direction. *Perception*, 38, 109–132, doi:10.1068/pp.5930.
- Tomassini, A., Morgan, M. J., & Solomon, J. A. (2010). Orientation uncertainty reduces perceived obliquity. *Vision Research*, 50, 541–547, doi:10.1016/j.visres.2009.12.005.
- Wei, X., & Stocker, A. A. (2015). A Bayesian observer model constrained by efficient coding can explain ‘anti-Bayesian’ percepts. *Nature Neuroscience*, 18, 1509–1517, doi:10.1038/nn.4105.
- Wollaston, W. H. (1824). On the apparent direction of eyes in a portrait. *Philosophical Transactions of the Royal Society of London*, 114, 247–256.